Synthesis of Poly(*p*-phenylene diamine) and Its Corrosion Inhibition Effect on Iron in 1*M* HCl

P. Manivel,[1] S. Sathiyanarayanan,[2] G. Venkatachari[2]

[1]*A. C. College of Engineering and Technology, Karaikudi 630 004, India*
[2]*Central Electrochemical Research Institute, Karaikudi 630 006, India*

Received 9 August 2007; accepted 26 May 2008
DOI 10.1002/app.28772
Published online 27 August 2008 in Wiley InterScience (www.interscience.wiley.com).

ABSTRACT: Water-soluble poly(*p*-phenylene diamine) was chemically synthesized. Its corrosion inhibition performance was evaluated for iron corrosion in 1*M* HCl at various concentrations, and the results were compared with that of the monomer. The corrosion inhibition properties were evaluated by polarization techniques and electrochemical impedance spectroscopy. The results showed that poly(*p*-phenylene diamine) was a more efficient corrosion inhibitor than the monomer and gave an 85% inhibition efficiency at a concentration of 50 ppm, whereas the monomer gave an efficiency of 73% at 5000 ppm. © 2008 Wiley Periodicals, Inc. J Appl Polym Sci 110: 2807–2814, 2008

Key words: adsorption; conjugated polymers; FT-IR

INTRODUCTION

The inhibition of corrosion in metals is of high technological importance,[1] and progress made in this field has been phenomenal in last few decades.[2,3] Acids find immense applications in pickling, cleaning, descaling, and so on. To avoid base-metal attack and to ensure the removal of corrosion products/scales alone, inhibitors are used extensively. The selection of appropriate inhibitors mainly depends on the type of acid, its concentration, temperature, velocity, presence of dissolved solids, and type of metallic materials involved. An important criterion in the characterization of the efficiency of inhibitors is their efficiency/concentration ratio. Schmitt,[4] in his review, discussed extensively the types of inhibitors recommended for the protection of metallic materials, especially ferrous metals and alloys, from corrosion in acid solutions during picking, acid cleaning, scale removing, and oil and gas well acidizing.

The important prerequisites for a compound to be an efficient inhibitor are (1) it should form a defect-free, compact barrier film; (2) it should chemisorb on to the metal surface; (3) it should be polymeric or polymerize *in situ* on the metal; and (4) the barrier thus formed should increase the inner layer thickness. Compounds containing nitrogen, sulfur, and oxygen have been established as good inhibitors for iron in acidic media.[5] Organic compounds having π bonds are found to inhibit corrosion steel by getting adsorbed over the electrode surface through electron sharing.[6] The presence of functional groups such as =NH, —N=N—, —CHO, R—OH, and R=R in the inhibitor molecule[7,8] and also the steric factors, aromaticity, and electron density at the donor atoms have been found to influence the adsorption of the inhibitor molecule over the corroding electrode surface. The role of the molecular area[9] and molecular weight[10] of the organic molecule on its inhibition efficiency has also been reported.

Various organic compounds, such as amines, acetylenic alcohols, and heterocyclic compounds, have been in use as inhibitors in industry.[11–15] In recent days, polymers[16] and conducting polymers[17–22] have attracted a great deal of attention because of their wide range of industrial applications and economics. Because of the presence of extensive delocalization of π electrons, these polymers could serve as better corrosion inhibitors at very low concentrations. Earlier studies[23–26] showed that substituents such as —OCH_3, —COOH, and —CH_3 present in polyaniline have a significant influence on the corrosion inhibitive properties for iron in 1*M* HCl. The order of inhibitor performance has been found to be Poly(*p*-anisidine) > Poly(*p*-amino benzoic acid) ≈ Poly(*p*-toludene) > Polyaniline. In this article, the effect of the NH_2 group on the corrosion inhibition of polyaniline for iron in 1*M* HCl is presented.

EXPERIMENTAL

Chemical synthesis of water-soluble poly(*p*-phenylene diamine) (PPD)

Reagent-grade *p*-phenylene diamine was used for the preparation of water-soluble PPD. A fresh 0.1*M*

Correspondence to: G. Venkatachari (gvchari@gmail.com).

Journal of Applied Polymer Science, Vol. 110, 2807–2814 (2008)

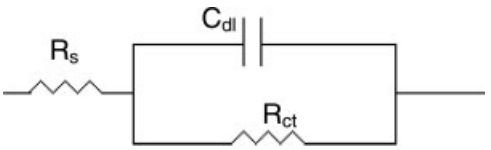

Scheme 1

solution of *p*-toluene sulfonic acid was prepared with double-distilled water. To this solution, 0.1*M* *p*-phenylene diamine (in 0.1*M* HCl) was added, and the solution was precooled to 0.5°C in a bath of ice and salt mixture. To this solution mixture, a freshly prepared solution of 0.1*M* ammonium persulfate was added slowly with constant stirring. The reaction temperature was maintained at 5 ± 2°C, and stirring was continued for 2 h to ensure the completion of the reaction.

Characterization of PPD

The synthesized PPD was characterized by ultraviolet–visible (UV–vis) spectroscopy (Hitachi, Model U 3400, Tokyo, Japan) and Fourier transform infrared (FTIR) spectroscopy (PerkinElmer Paragon 500). The molecular weight determination was carried out by gel permeation chromatography (Shimadzu, Kyoto, Japan).

Electrochemical measurements

Pure iron (99.998%) was used as a test electrode, and it was embedded in Araldite, so as to expose a surface area of 1 cm^2. The electrode was polished successively on emery papers of grade 1/0, 2/0, 3/0, and 4/0 and then degreased with trichloroethylene. The electrochemical studies were carried out with a double-walled glass cell with a capacity of 200 mL and with provisions for the working electrode, platinum counter electrode, and luggin capillary. The potential of the working electrode was measured with respect to a saturated calomel electrode (SCE) through the luggin capillary. The experiments were carried out after the steady-state attainment of corrosion potentials (15 min) at 30 ± 1°C. All of the solutions were prepared with reagent-grade chemicals in double-distilled water.

The experiments were conducted with a Solartron electrochemical measurement unit (model 1280 B, Solartron Analytical, Hampshire, England) with the software packages Z Plot 2 for impedance measurements and Corr Ware 2 for polarization measurements, Solartron Analytical, Hampshire, England. This system included a potentiostat, a built-in lock-in analyzer, and a personal computer. Impedance measurements were carried out at corrosion potential with an alternating-current amplitude of 20 mV for the frequency range 10 KHz–10 mHz. The real (Z') and imaginary (Z'') parts of the impedance were plotted in Nyquist plots. From the Nyquist plots, the charge-transfer resistance (R_{ct}) and interfacial double-layer capacitance (C_{dl}) values were calculated by the assumption of the equivalent circuit shown in Scheme 1 and fitting of the experimental data.

The inhibition efficiency of the inhibitor was determined from the R_{ct} values with the following equation:

$$\text{Inhibition efficiency}(\%) = \frac{R'_{ct} - R_{ct}}{R'_{ct}} \times 100 \qquad (1)$$

where R_{ct} and R'_{ct} are the charge-transfer resistances in the absence and presence of inhibitors, respectively.

The C_{dl} value was estimated from the impedance value of the frequency having the maximum imaginary component (f_{max}) in the Nyquist plot with the following equation:

$$C_{dl} = \frac{1}{2\pi f_{max} R_{ct}} \qquad (2)$$

The surface coverage (θ) by the inhibitor molecule was given by

$$\theta = \frac{C_{dl} - C'_{dl}}{C_{dl} - C_{dls}} = \frac{C_{dl} - C'_{dl}}{C_{dl}} \qquad (3)$$

because $C_{dls} \ll C_{dl}$. Here, C_{dl}, C'_{dl} and C_{dls} are the double-layer capacitance values in the absence and presence of inhibitors and the saturated double-layer capacitance value in the presence of the inhibitor, respectively.[27–29]

For linear polarization resistance studies, the measurements were carried out within the potential range −20 to +20 mV with respect to the open-circuit potential, and the current response was

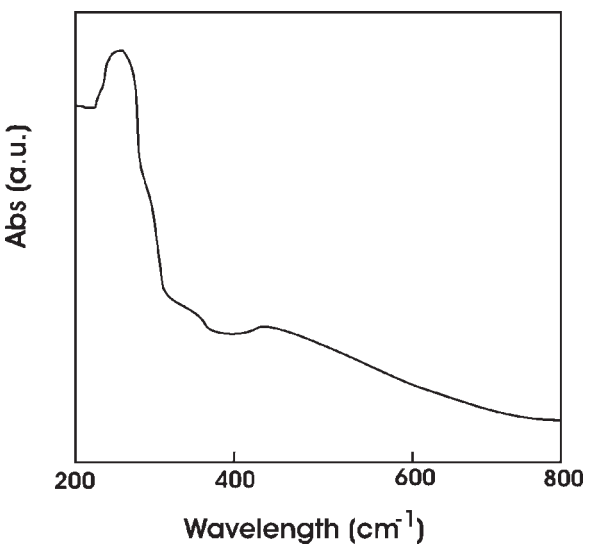

Figure 1 UV–vis spectrum of PPD.

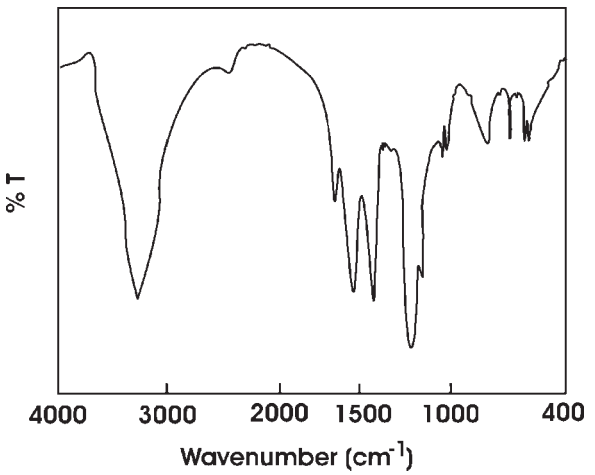

Figure 2 FTIR spectrum of PPD.

measured at a scan rate of 0.5 mV/s. The overpotential and current data were plotted on a linear scale to get linear polarization resistance (LPR) plots, and the slope of the plots in the vicinity of the corrosion potential gave the polarization resistance (R_p). From the measured R_p values, the inhibition efficiency (%) was calculated with the following relationship:

$$\text{Inhibition effeciency } (\%) = \frac{R'_p - R_p}{R'_p} \times 100 \qquad (4)$$

where R_p and R'_p are the polarization resistance values without and with the addition of inhibitors.

For potentiodynamic polarization studies, the experiments were carried out over the potential range −200 to +200 mV with respect to the open-circuit potential at a scan rate of 0.5 mV/s. By extrapolating the tafel regions to the corrosion potential, we obtained the various corrosion kinetic parameters, such as the corrosion current (i_{corr}), corrosion potential (E_{corr}), anodic tafel slope (b_a) and cathodic tafel slope (b_c), from these polarization curves. The inhibition efficiency was evaluated from the measured i_{corr} values with the following relationship:

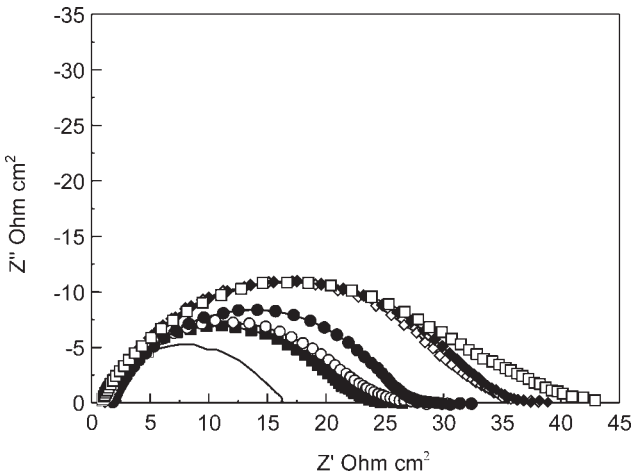

Figure 3 Impedance behavior of iron in 1*M* HCl with the addition of *p*-phenylene diamine: (—) blank, (■) 100 ppm, (○) 500 ppm, (●) 750 ppm, (◇) 1000 ppm, (◆) 2500 ppm, and (□) 5000 ppm.

$$\text{Inhibition effeciency } (\%) = \frac{i_{corr} - i'_{corr}}{i_{corr}} \times 100 \qquad (5)$$

where i_{corr} and i'_{corr} are the corrosion current values without and with the addition of various concentrations of inhibitor.

The morphologies of the iron surface after corrosion in the presence and absence of inhibitor in 1*M* HCl under a magnification of 100× were examined by scanning electron microscopy (Hitachi S 3000H).

RESULTS AND DISCUSSION

Characterization of PPD

The UV–vis spectrum of PPD is shown in Figure 1. The absorption peak at 330 nm showed the π–π* transition in the benzenoid ring. The well-known cation radicals and localized polaron peaks were observed at 420 nm.[30]

The FTIR spectrum of PPD is given in Figure 2. The spectra was similar to that of polyaniline: (1) the

TABLE I
Electrochemical Impedance and Linear Polarization Parameters for Pure Iron in 1*M* HCl Containing *p*-Phenylene Diamine

	Impedance method				LPR method	
Concentration (ppm)	R_{ct} (Ω cm^2)	C_{dl} (μF/cm^2)	Inhibition efficiency (%)	θ	R_p (Ω cm^2)	Inhibition efficiency (%)
0	15.6	330.1	—	—	17.4	—
100	23.5	176.5	33.9	0.47	36.1	51.8
500	24.8	176.5	37.3	0.47	40.5	57.1
750	27.7	167.0	43.8	0.49	40.2	56.7
1000	34.3	153.1	54.7	0.54	50.6	65.6
2500	35.6	140.0	56.3	0.58	48.3	64.0
5000	40.4	107.5	61.5	0.67	48.7	64.3

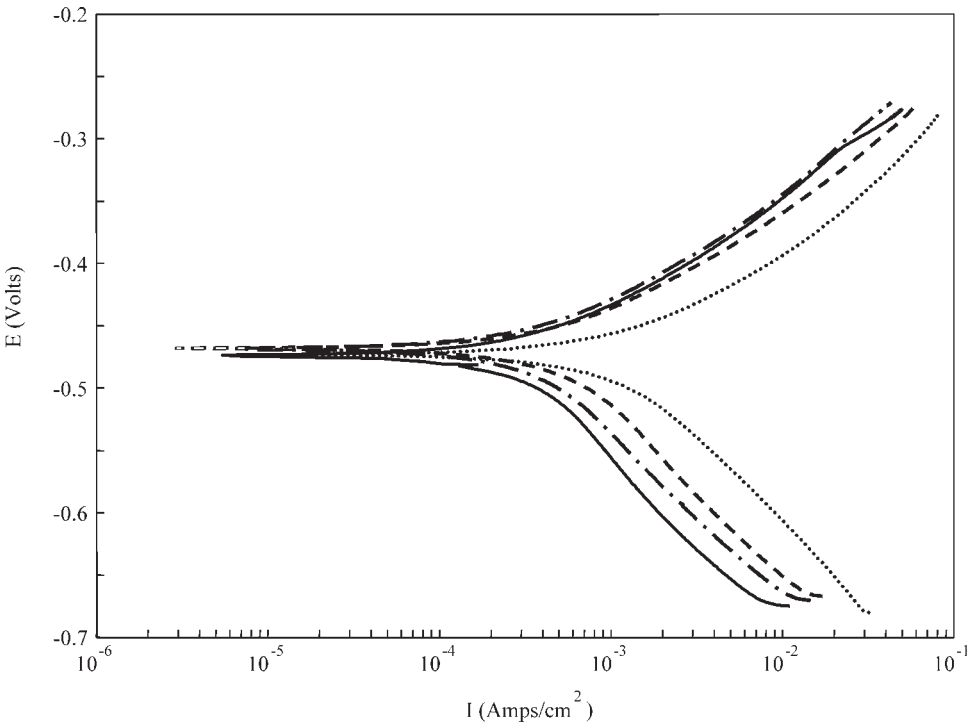

Figure 4 Potentiodynamic polarization behavior of iron in 1*M* HCl with the addition of *p*-phenylene diamine: (· · ·) blank, (- - -) 100 ppm, (– · –) 1000 ppm, and (—) 5000 ppm (I = current; E = potential).

bands at 1570 and 1508 cm^{-1} were assigned to quinoid and benzenoid rings, (2) the band at 816 cm^{-1} was due to 1,4-substituted benzene, and (3) the band at 1124 cm^{-1} was due to the bending vibration of C—H, which was formed during protonation.[31,32] The molecular weight of PPD was found to be 55,138. The structure of PPD is reported as follows:[33,34]

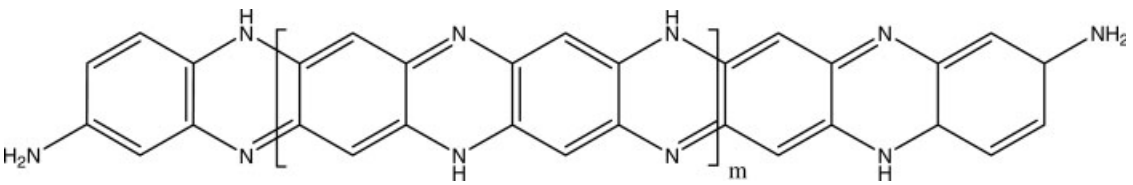

TABLE II
Corrosion Kinetic Parameters of Pure Iron in 1*M* HCl Containing *p*-Phenylene Diamine

Concentration (ppm)	E_{corr} (mV) versus SCE	Tafel slopes (mV/dec)		i_{corr} (μA/cm^2)	Inhibition efficiency (%)
		b_a	b_c		
0	− 488.4	99.7	133.1	1425.5	—
100	− 468.1	88.7	146.1	665.5	53.3
500	− 470.8	85.3	129.6	551.9	61.3
750	− 471.6	98.6	136.5	502.1	64.8
1000	− 471.6	87.9	136.8	460.3	67.7
2500	− 471.8	92.5	137.5	403.4	71.7
5000	− 475.6	93.4	155.6	390.1	72.6

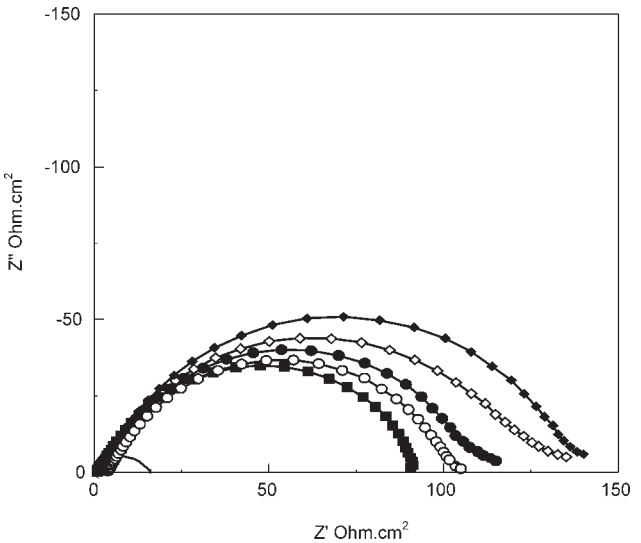

Figure 5 Impedance behavior of iron in 1*M* HCl with the addition of PPD: (—) blank, (■) 25 ppm, (○) 50 ppm, (●) 100 ppm, (◇) 250 ppm, and (◆) 500 ppm.

A similar structure was proposed for poly(*o*-phenylene diamine).[35]

Corrosion inhibition by *p*-phenylene diamine

The Nyquist representations of the impedance behavior of iron in 1*M* HCl with and without the addition of various concentrations of *p*-phenylene diamine are shown in Figure 3. The existence of a single semicircle showed the presence of a single charge-transfer process during dissolution, which was unaffected by the presence of inhibitor molecules. The slightly depressed nature of the semicircle, which had the center below the *x* axis, is characteristic for solid electrodes, and such frequency dispersion has been attributed to microroughness and other inhomogeneties of the solid electrode.[36–38] The R_{ct} and C_{dl} values derived from these curves are given in Table I. R_{ct} increased from 15.6 to 40.4 Ω cm^2, and C_{dl} decreased from 330.1 to 107.5 μF/cm^2 with the addition of *p*-phenylene diamine inhibitor.

The potentiodynamic polarization behavior of iron in 1*M* HCl with the addition of various concentrations of *p*-phenylene diamine in the tafel region is shown in Figure 4. The corrosion kinetic parameters derived from these curves are given in Table II. As shown in Table II, it is clear that the addition of *p*-phenylene diamine in the concentration range 100–5000 ppm decreased the dissolution rate of iron in 1*M* HCl. The i_{corr} value decreased from 1426 μA/cm^2 for the inhibitor-free solution to 390 μA/cm^2 to yield a 64.3% inhibition efficiency at the highest concentration of *p*-phenylene diamine studied.

The steady-state corrosion potentials shifted by 15 mV in the anodic direction in the presence of inhibitor. In addition, the anodic and cathodic tafel slopes were in the ranges 85 ± 5 mV and 125 ± 5 mV, respectively. Because there was no remarkable change in the corrosion potential and tafel slopes in the presence of inhibitor, we inferred that *p*-phenylene diamine was a mixed inhibitor.

The R_p values showed (Table I) an increase in values from 17.4 to 48.7 Ω cm^2 with the addition of *p*-phenylene diamine inhibitor.

Amines in aqueous acidic solutions may exist as either neutral molecules or in the form of cations,[39] depending on the concentration of H^+ ions in the solution. In acidic chloride solutions, the amines adsorb through electrostatic interaction between the positively charged anilinium cation and the negatively charged metal surface because of the specific adsorption of chloride on the metal.[40] Moreover, in aromatic amines, the interaction between the π electrons of the benzene ring and the positively charged metal surface also plays a role.[41] Murakawa and Hackerman[42] suggested that the stronger adsorption of organic molecules is not always a direct combination of organic molecules with the metal surface, but in some cases, it occurs through already adsorbed sulfate ions, which interfere with the adsorption of organic molecules. The adsorption of the inhibitor molecules can be visualized predominantly as

TABLE III
Electrochemical Impedance and Linear Polarization Parameters for Pure Iron in 1*M* HCl Containing PPD

	Impedance method				LPR method	
Concentration (ppm)	R_{ct} (Ω cm^2)	C_{dl} (μF/cm^2)	Inhibition efficiency (%)	θ	R_p (Ω cm^2)	Inhibition efficiency (%)
0	15.6	330.1	—	—	17.4	—
25	91.6	173.7	82.9	0.47	102.8	83.1
50	98.6	171.6	84.1	0.48	116.0	85.0
100	109.3	164.0	85.7	0.44	132.0	86.8
250	127.7	136.3	87.8	0.59	150.6	88.4
500	136.7	96.6	88.6	0.70	152.9	88.6

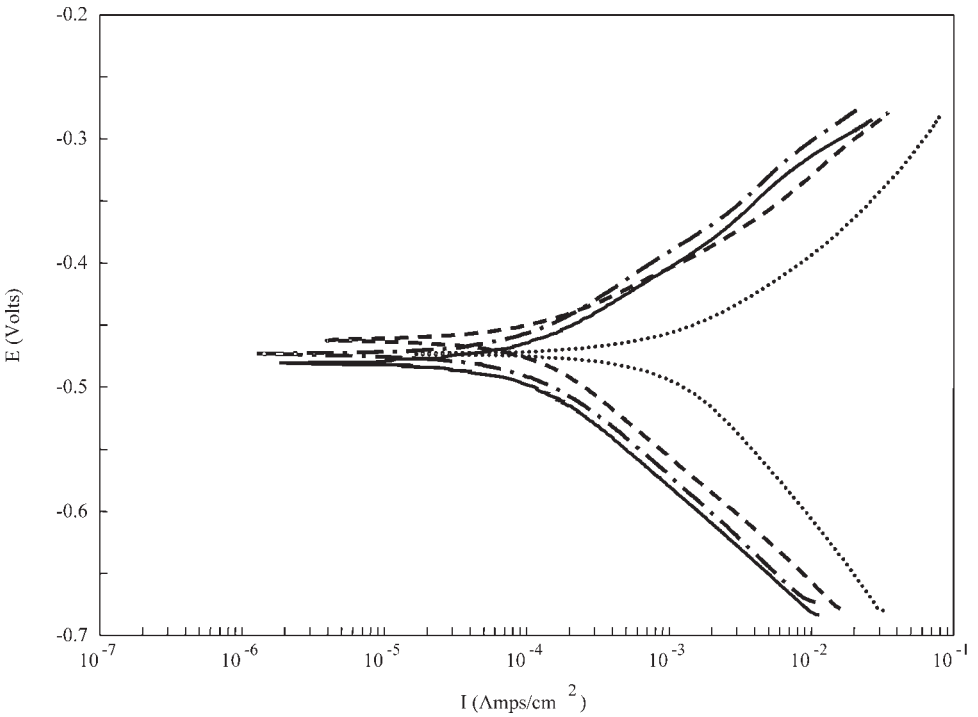

Figure 6 Potentiodynamic polarization behavior of iron in 1*M* HCl with the addition of PPD: (· · ·) blank, (- - -) 25 ppm, (– · –) 100 ppm, and (—) 500 ppm (I = current; E = potential).

RNH_3^+ ions lying flat on the electrode surface, with the principal adsorption forces arising from a π-bond orbital, as reported by Blomgren and Bockris.[43]

Corrosion inhibition by PPD

It is expected that compounds with a higher molecular weight and bulky structure may cover more area on an active electrode surface.[44] If such a bulky molecule can have chemisorptive properties, it is naturally expected to inhibit corrosion more effectively.

The impedance behavior of the PPD-containing solution is shown in the Nyquist diagram (Fig. 5). R_{ct}, C_{dl}, and hence θ derived from these figures, as explained previously, are given in Table III. The R_{ct} values increased from 15.6 to 136.7 Ω cm^2 with a corresponding decrease in C_{dl} values from 330.1 to 96.6 μF/cm^2 for the added PPD concentrations. A decrease in C_{dl}, which could have resulted from a decrease in the local dielectric constant and/or an increase in the thickness of the electrical double layer, suggested that the inhibitors adsorbed at the metal–solution interface.[45]

Figure 6 shows the tafel polarization curves for iron in 1*M* HCl with the addition of various concentrations of PPD. The important corrosion parameters obtained from these curves are presented in Table IV. It is evident from the table that the i_{corr} values decreased from 1425.5 μA/cm^2 for the blank to 103.7 μA/cm^2 with the addition of the highest concentration of PPD. This can be compared with the high value of 390 μA/cm^2 obtained with the

TABLE IV
Corrosion Kinetic Parameters of Pure Iron in 1*M* HCl Containing PPD

Concentration (ppm)	E_{corr} (mV) versus SCE	Tafel slopes (mV/dec)		i_{corr} (μA/cm^2)	Inhibition efficiency (%)
		b_a	b_c		
0	− 488	99.7	133.1	1425.5	—
25	− 479	76.5	96.50	143.5	89.9
50	− 480	75.5	94.20	134.5	90.5
100	− 481	79.4	96.80	125.4	91.2
250	− 484	84.7	98.80	111.7	92.1
500	− 474	81.0	100	103.7	92.7

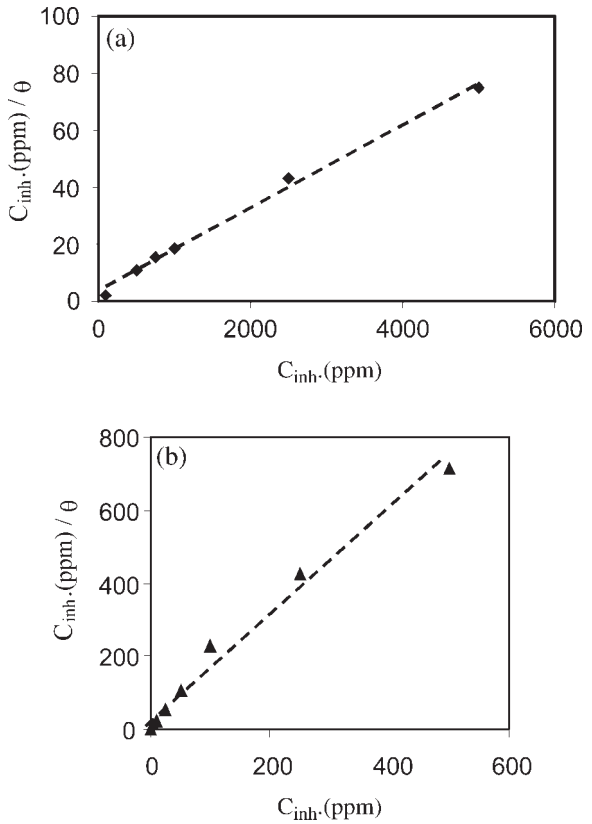

Figure 7 Langmuir adsorption isotherm plots for (a) *p*-phenylene diamine and (b) PPD.

addition of 5000 ppm of the *p*-phenylene diamine monomer. The addition of PPD did not alter the values of E_{corr}, b_a, and b_c significantly, which indicated a mixed-type inhibiting behavior of the added inhibitor.

From the LPR studies too, we found that the R_p values (Table III) increased from 17.4 Ω cm^2 for the blank to 152.9 Ω cm^2 with the highest concentration of inhibitor added, which indicated the good inhibition characteristics of the added PPD.

The inhibitive effect of substituted anilines[17,18] and polyaniline[20] for mild steel in acid chloride solutions were very high because of the presence of extensive delocalized π electrons, quaternary nitrogen, and bulky molecular size. The bulky molecular size ensured the greater coverage of the active surface, whereas the earlier ones took care of the adsorption over the corroding surface. The inhibitive properties of PPD were also due to the presence of extensive delocalized π electrons, quaternary nitrogen, and a larger molecular size. The adsorption of amine molecules on the metal surface took place in the form of (1) a neutral molecule through chemisorption, involving the sharing of electrons between nitrogen and iron atoms; (2) π electron interaction with the metal surface; or (3) the adsorption of the cationic form of the polymer on the chloride-adsorbed iron surface. Of these, the adsorption through the cationic form was more probable because amines exist in a protonated cationic form in acid media.[36,39]

Figure 7 shows the adsorption isotherms [a plot of inhibitor concentration C_{inh} vs (C_{inh}/θ)] for the *p*-phenylene diamine and PPD, respectively. The linear relationship of the plots showed that *p*-phenylene diamine and PPD inhibited the corrosion of iron in 1*M* HCl by adsorption according to Langmuir adsorption and, hence, retarded anodic dissolution and cathodic hydrogen evolution reactions. When we compared it to the inhibitor performance of polyaniline,[26] we found that PPD gave a higher corrosion inhibition for iron in 1*M* HCl.

The scanning electron microscopy photographs with 100× magnification for iron in 1*M* HCl with and without the presence of PPD are given in Figure 8(a,b). We observed from the photographs that attack in the presence of PPD in 1*M* HCl was much less common in comparison with attack in the absence of the inhibitor-free acid solution.

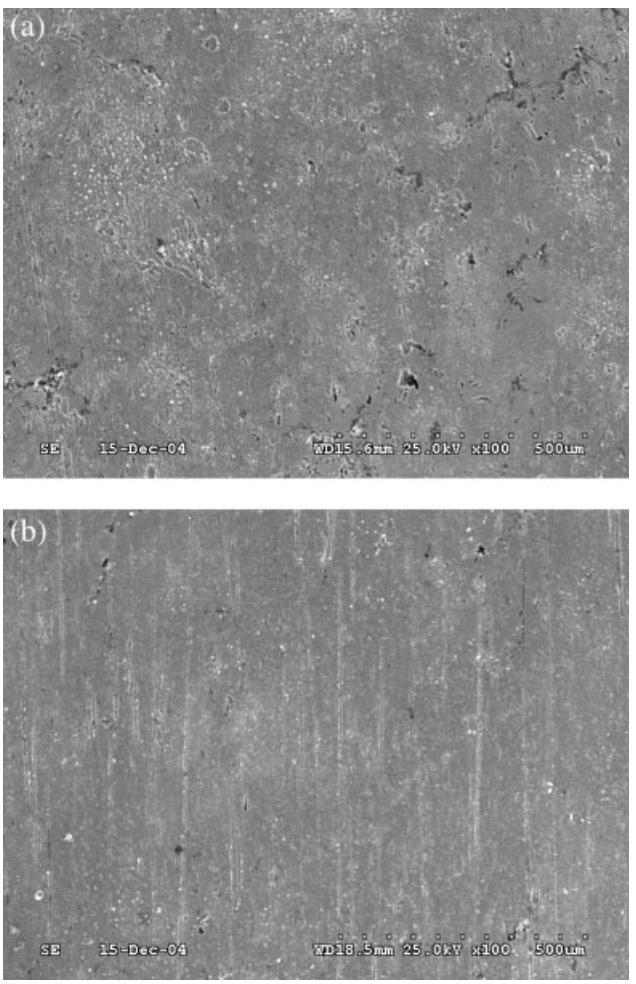

Figure 8 Scanning electron micrographs of iron in 1*M* HCl: (a) without the inhibitor and (b) with PPD.

CONCLUSIONS

Water-soluble PPD was synthesized by a chemical polymerization route, and its corrosion inhibition performance was evaluated for iron in 1*M* HCl. The results indicated that PPD behaved as mixed type of inhibitor and yielded more than 90% inhibition efficiency. The adsorption of monomer and PPD on the iron surface obeyed Langmuir's adsorption isotherm.

The authors thank the director of Central Electrochemical Research Institute (CECRI) (Karaikudi, India) for his kind permission.

References

1. Ali, S. A.; Saeed, M. T.; Rahman, S. V. Corros Sci 2003, 45, 253.
2. Sastry, V. S. Corrosion Inhibitors—Principles and Application; Wiley: West Sussex, England, 1998.
3. Nathan, C. C. Corrosion Inhibitors; NACE: Houston, 1973.
4. Schmitt, G. Br Corros J 1984, 19, 165.
5. Lagrnee, M.; Mernari, B.; Bouanis, M.; Traisnel, M.; Bentiss, F. Corros Sci 2002, 44, 573.
6. Bentiss, F.; Lagrenee, M.; Traisnel, M.; Hornez, J. C. Corros Sci 1999, 41, 789.
7. Growcok, F. B.; Frenier, W. W.; Andrezzi, P. A. Corrosion 1989, 45, 1007.
8. Lukovits, I.; Kalman, E.; Palinkas, G. Corrosion 1995, 51, 201.
9. Ayers, R. C., Jr.; Hackerman, N. J Electrochem Soc 1963, 110, 507.
10. Trabanelli, G.; Zucchi, F. Rev Coat Corros 1972, 1, 97.
11. Lewis, G. Corros Sci 1982, 22, 579.
12. Rengamani, S.; Vasudevan, T.; Venkatakrishna Iyer, S. Ind J Technol 1993, 31, 519.
13. Muralidharan, S.; Quraishi, M. A.; Venkatakrishna Iyer, S. Ind J Chem Technol 1994, 1, 168.
14. Sekine, I.; Sanbongi, M.; Hagiuda, H.; Oshibe, T.; Yusa, M.; Imahama, T.; Shibata, Y.; Wake, T. J Electrochem Soc 1992, 139, 3167.
15. Bartos, M.; Hackerman, N. J Electrochem Soc 1992, 139, 3428.
16. Joshi, A.; Srivastava, K. Corros Prev Control 1989, 36, 138.
17. Sathiyanarayanan, S.; Dawan, S. K.; Trivedi, D. C.; Balakrishnan, K. Corros Sci 1992, 33, 1831.
18. Sathiyanarayanan, S.; Dawan, S. K.; Trivedi, D. C.; Balakrishnan, K. Electrochim Acta 1994, 39, 831.
19. Jeyaprabha, C.; Sathiyanarayanan, S.; Phani, K. L. N.; Venkatachari, G. J Electroanal Chem 2005, 585, 157.
20. Jeyaprabha, C.; Sathiyanarayanan, S.; Venkatachari, G. J Appl Polym Sci 2006, 101, 2144.
21. Jeyaprabha, C.; Sathiyanarayanan, S.; Venkatachari, G. J Electroanal Chem 2005, 583, 232.
22. Jeyaprabha, C.; Sathiyanarayanan, S.; Phani, K. L. N.; Venkatachari, G. Appl Surf Sci 2005, 252, 966.
23. Manivel, P.; Venkatachari, G. Corros Sci Technol (Korea) 2005, 4, 6.
24. Manivel, P.; Venkatachari, G. J Mater Sci Technol 2006, 22, 7.
25. Manivel, P.; Venkatachari, G. J Appl Polym Sci 2007, 104, 2595.
26. Manivel, P.; Sathiyanarayanan, S.; Venkatachari, G. J Appl Polym Sci 2007, 106, 3988.
27. Elkadi, L.; Menari, B.; Traisnel, M.; Bentiss, F.; Lagrenee, M. Corros Sci 2000, 42, 703.
28. Rengamani, S.; Iyer, S. V. K. J Appl Electrochem 1994, 24, 355.
29. Mernari, B.; Attari, H. E. L.; Traisnel, M.; Bentiss, F.; Lagrenee, M. Corros Sci 1998, 48, 391.
30. Zhang, L. J.; Wan, M. X. J Phys Chem B 2003, 107, 6748.
31. Tang, S.; Jing, X. B.; Wang, B. C.; Wang, F. Synth Met 1988, 24, 231.
32. Cao, Y.; Li, S.; Xue, Z.; Guo, D. Synth Met 1986, 16, 305.
33. Li, X.-G.; Huang, M.-R.; Chen, R.-F.; Jin, Y.; Yang, Y.-L. J Appl Polym Sci 2001, 81, 3107.
34. Cataldo, F. Eur Polym J 1996, 32, 43.
35. Kraljic, M.; Zic, M.; Duie, L. Bull Electrochem 2004, 20, 567.
36. Jutner, K. Electrochim Acta 1990, 35, 1150.
37. Paskossy, T. J Electroanal Chem 1994, 364, 111.
38. Fawcet, W. R.; Kovacova, Z.; Motheo, A.; Foss, C. J Electroanal Chem 1992, 326, 91.
39. Mann, C. A. Trans Electrochem 1936, 69, 105.
40. Gerovich, M. A.; Rybalchenko, G. F. Zh Fiz Khim 1958, 32, 109.
41. Antropov, L. I. Int Congress Met Corros 1963, 1, 147.
42. Murakawa, T.; Hackerman, N. Corros Sci 1964, 4, 387.
43. Blomgren, E.; Bockris, J. O. M. J Phys Chem 1959, 63, 1475.
44. Ayers, R. C., Jr.; Hackerman, N. J Electrochem Soc 1963, 110, 507.
45. McCafferty, E.; Hackerman, N. J Electrochem Soc 1972, 119, 146.